HOKKAIDO UNIVERSITY

Title	Basic [Au-25(SCH2CH2Py)(18)](-).Na+ Clusters: Synthesis, Layered Crystallographic Arrangement, and Unique Surface Protonation
Author(s)	Huang, Zhong; Ishida, Yohei; Yonezawa, Tetsu
Citation	Angewandte chemie-international edition, 58(38), 13411-13415 https://doi.org/10.1002/anie.201908905
Issue Date	2020-09-16
Doc URL	https://hdl.handle.net/2115/79273
Rights	This is the peer reviewed version of the following article: Z. Huang, Y. Ishida, T. Yonezawa, Angew. Chem. Int. Ed. 2019, 58, 13411. , which has been published in final form at Z. Huang, Y. Ishida, T. Yonezawa, Angew. Chem. Int. Ed. 2019, 58, 13411. . This article may be used for non-commercial purposes in accordance with Wiley Terms and Conditions for Use of Self-Archived Versions.
Type	journal article
File Information	Supporting information-revised-Angew Chemie.pdf

Hokkaido University Collection of Scholarly and Academic Papers : HUSCAP

Supporting Information

Basic $[Au_{25}(SCH_2CH_2Py)_{18}]^{-}\cdot Na^{+}$ Clusters: Synthesis, Layered Crystallographic Arrangement and Unique Surface Protonation

Zhong Huang, Yohei Ishida, and Tetsu Yonezawa**

Table of Contents

I. Experimental section **3**

I.1 Chemicals. 3

I.2 Synthesis and purification of $[Au_{25}(PyET)_{18}]^-$ clusters 3

I.3 Crystallization and X-ray crystallographic determination of $[Au_{25}(PyET)_{18}]^- \cdot Na^+$ clusters. 4

I.4 Protonation reaction on $[Au_{25}(PyET)_{18}]^-$ clusters. 4

I.5 Characterization. 5

II. Characterizations of the samples (Figure S1−S4) **6**

III. Crystal results of $[Au_{25}(PyET)_{18}]^- \cdot Na^+$ and $[Au_{25}(PET)_{18}]^- \cdot TOA^+$ clusters (Figure S5−S11 and Table S1−S3) **9**

IV. Titrations results of $[Au_{25}(4\text{-}PyET)_{18}]^-$ clusters (Figure S12−S20 and Table S4−S5) **17**

V. Reversible (de)protonation of $[Au_{25}(PyET)_{18}]^-$ clusters (Figure S21−S22 and Table S6) **28**

VI. References **30**

I. Experimental section

I.1 Chemicals. Hydrogen tetrachloroaurate (III) ($HAuCl_4 \cdot 4H_2O$, >99.99%, Wako, Japan), 2-(4-pyridinyl)ethanethiol hydrochloride (4-PyET·HCl, >97%, TCI, Japan), 2-pyridyl ethylmercaptan (2-PyET, TRC, Canada), phenyl ethanethiol (PET, 99%, Wako, Japan), tetra-*n*-octylammonium bromide (TOABr, >98%, Wako, Japan), sodium borohydride ($NaBH_4$, 99%, Wako, Japan), sodium hydroxide (NaOH, >97%, Junsei, Japan), hydrochloric acid (HCl, 35−37%, Kanto, Japan), hydrogen chloride–methanol solution (HCl–MeOH, ~1.25 M, Aldrich), acetic acid (CH_3COOH, >99.7%, Junsei, Japan), deuterium chloride solution (DCl, 35 wt.% in D_2O, Aldrich) and sodium deuteroxide solution (NaOD, 40 wt.% in D_2O, Aldrich) were used as received without further purification. HPLC-grade solvents such as tetrahydrofuran (THF), methanol (MeOH), dimethylformamide (DMF), and dichloromethane (DCM) were purchased from Kanto, Japan. Deionized pure water (>18.2 MΩ) was prepared by an Organo/ELGA purelab system.

I.2 Synthesis and purification of $[Au_{25}(PyET)_{18}]^-$ clusters. Solutions of $HAuCl_4$ (6.7 mM, stock solution) and 4-PyET (100.0 mM, stock solution) were separately prepared with THF and MeOH. In a typical synthesis of $[Au_{25}(4\text{-PyET})_{18}]^-$ clusters, 8 mL of the 4-PyET solution was added dropwise into 24 mL of the $HAuCl_4$ solution (noted the ratio of THF to MeOH was 3:1 by volume, and the ratio of 4-PyET to Au was 5:1 by mole) under stirring. The mixture changed into a light reddish turbid suspension, and then into a white turbid suspension during the addition of 4-PyET. After stirring overnight, white residues were found to stick to the inner wall of the flask. The white residues could be redispersed completely by sonication for 1 min to form a turbid suspension again. Then, 1.6 mL of the freshly prepared $NaBH_4$ aqueous solution (1.6 mmol, 10:1 molar ratio of $NaBH_4$ to Au, prepared by dissolving 189.2 mg of $NaBH_4$ in 5 mL of cold pure water) was rapidly added to the suspension under vigorous stirring. The color of the suspension immediately turned black, indicating the formation of Au_m clusters. After approximately 1 h of vigorous stirring, the color became slight brownish. The stirring rate was decreased to 500 rpm and the etching process was allowed to continue for at least 48 h. During the long-time etching process, the solution color slowly changed to dark brown, which suggested that the crude polydisperse Au_m clusters were converted to monodisperse $[Au_{25}(4\text{-PyET})_{18}]^-$ clusters.

To determine the optimized preparation of $[Au_{25}(4\text{-PyET})_{18}]^-$, we obtained results for different volume ratios of THF to MeOH (including 0:1, 1:7, 1:3, 1:1, 7:1, and 1:0) and molar ratios of $HAuCl_4$ to 4-PyET (including 1:20, 1:10, 1:3, 1:1) as well as $HAuCl_4$ to $NaBH_4$ (including 1:50, 1:20, 1:5, and 1:2). The $[Au_{25}(2\text{-PyET})_{18}]^-$ clusters were prepared though the same synthetic strategy except that the

concentrations of $HAuCl_4$ and 2-PyET solutions were changed into 1.7 mM and 25.0 mM, respectively, and the etching time was set at 10 h.

The crude sample was cleaned first by centrifugation to remove any solids. Then, under stirring, 2 mL of aqueous HCl (375.0 mM) was rapidly added to the crude sample and the brownish precipitation was collected by centrifugation. The as-collected solid was washed by THF twice and then redissolved in 8 mL of MeOH. The insoluble particles were removed by centrifugation. In the as-obtained 8 mL of the Au_{25}-contained MeOH solution, 32 mL of aqueous NaOH solution (200.0 mM) was added (the ratio of MeOH to water was 1:4 by volume), which would deprotonate the pendant Py groups and simultaneously precipitate the Au_{25} clusters. Finally, the brown solid, collected by centrifugation, was washed by water thrice to remove the polydispersed Au clusters ($[Au(4\text{-}PyET)]_m$) and impurity ion (Cl^-). If the as-obtained products still contained $[Au(4\text{-}PyET)]_m$ (or Cl^-, which was detected in the form of $[Au_{25}(4\text{-}PyET)_{18}Cl]^{2-}$ by ESI-MS), they would be repeatedly dissolved in MeOH, precipitated by NaOH solution and washed by water, as same to the above process. The final purified products, $[Au_{25}(4\text{-}PyET)_{18}]^-\cdot Na^+$ or $[Au_{25}(2\text{-}PyET)_{18}]^-\cdot Na^+$, were stored in dry form or in DMF solution.

In addition, for comparison, $[Au_{25}(PET)_{18}]^-\cdot TOA^+$ clusters were prepared based on a method previously reported by Murray's group.[S1]

I.3 Crystallization and X-ray crystallographic determination of $[Au_{25}(PyET)_{18}]^-\cdot Na^+$ clusters. Recrystallization of $[Au_{25}(PyET)_{18}]^-\cdot Na^+$ was carried out by a vapor diffusion method. Fully deprotonated $[Au_{25}(4\text{-}PyET)_{18}]^-\cdot Na^+$ clusters were dispersed in DMF at a concentration of ~10.0 mg/mL (1.3 mM) in a 5-mL vial without a seal. The 5-mL vial containing the sample was placed in the middle of a separate 50-mL vial. Then, diethyl ether (non-solvent of clusters) was introduced into the 50-mL vial. After tightly sealing the 50-mL vial, it was kept in a refrigerator at 4 °C. After approximately 5–7 days, black belt-shaped crystals were successfully obtained and analyzed by X-ray diffraction (Figure S5). For comparison, $[Au_{25}(PET)_{18}]^-\cdot TOA^+$ crystals were also prepared based on the previous work by Jin's group.[S2] Details acquired on the crystal structure and refinement are shown in Tables S1 and S2.

I.4 Protonation reaction on $[Au_{25}(PyET)_{18}]^-$ clusters. In 3 mL aliquots of MeOH, each containing 100 μg/mL (0.013 mM) of $[Au_{25}(PyET)_{18}]^-$ clusters, 4.8, 9.6, 14.4, and 28.8 μL of the HCl–MeOH solution (500 mM) were added separately. Each batch was stirred at 300 rpm for 30 s and then subjected to UV-vis absorption characterization in a quartz cuvette with a 10-mm optical path. The reversible protonation–deprotonation process was studied in this part of the experiment by adding 9.6 μL of HCl solution and subsequently 14.4 μL of the NaOH–MeOH solution (500 mM). In NMR monitoring of the protonation, 1.0 mg (0.13 μmol) of $[Au_{25}(PyET)_{18}]^-\cdot Na^+$ clusters was dissolved in 0.6 mL of methanol-d_4, and then 16 μL aliquot of the DCl-D_2O solution (50 mM) was injected step-by-step and

immediately analyzed by ^{1}H-NMR. The masses for the free PyET titrations (2.4 μmol) were set equal to those of PyET ligands on the surface of $[Au_{25}(PyET)_{18}]^{-}\cdot Na^{+}$ clusters. The reversible protonation–deprotonation process under NMR investigation was conducted by adding 96 μL of the DCl-D_2O solution and subsequently 144 μL of the NaOD-D_2O solution (50 mM).

I.5 Characterization. UV-vis absorption spectra were recorded using a JASCO V-630 spectrophotometer. Electrospray-ionization mass spectrometry (ESI-MS) was performed using a Bruker Daltonics micrOTOF-HS mass spectrometer. The purified sample dissolved in methanol (~0.013 mM) was directly infused at 4 $mL\cdot min^{-1}$. The nebulizer pressure was set to 1.5 bar, and the sheath gas flow was set to 4.0 L/min. The dry temperature was maintained at 120 °C. The electrospray emitter potential was held at –4500 V (in the negative mode) and 4500 V (in the positive mode). The capillary exit, skimmer 1, hexapole 1, and skimmer 2 voltages were 200, 50, 25, and 28 V, respectively. The lens 1 transfer and lens 1 pre plus storage were set at 160 and 30 μs, respectively. Thermogravimetric analysis (TGA) was undertaken on a Shimadzu DTG-60H instrument in a N_2 atmosphere (flow rate: ~100 mL min^{-1}). The obtained pure $[Au_{25}(PyET)_{18}]^{-}\cdot Na^{+}$ was put into an alumina cell, and the temperature was increased to 600 °C at a heating rate of 5 °C min^{-1}. ^{1}H-NMR and COSY analyses were performed on a JMTC-400/54/SS (JEOL) spectrometer operating at 400 MHz. EDX analysis was performed using the crystal sample at a scanning electron microscopy (JEOL, JSM-6701F) equipped with the JEOL JED-2300 EDS system.

II. Characterizations of the samples

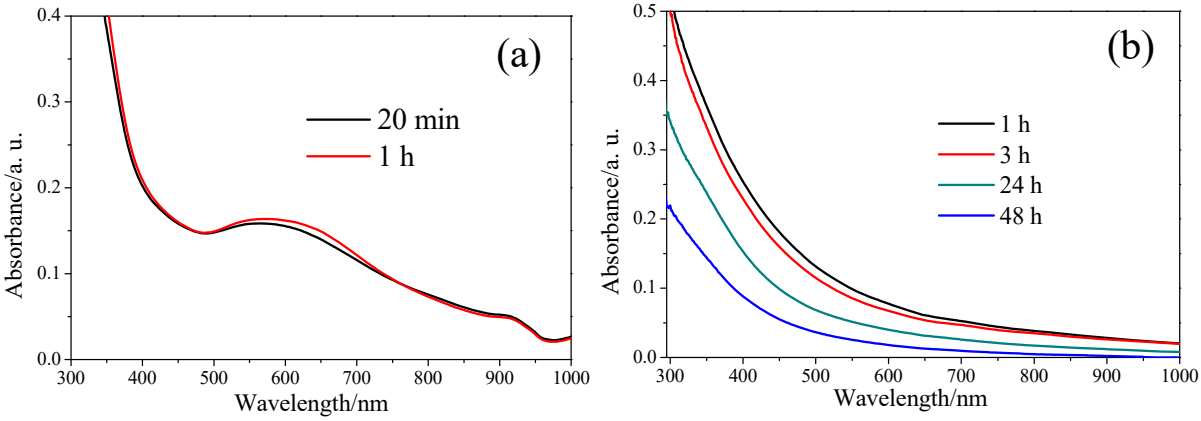

Figure S1. UV-vis absorption monitoring of the etching process of 4-PyET-protected Au_m clusters in: (a) MeOH solvent; (b) H_2O solvent (the molar ratios of $HAuCl_4$ to 4-PyET and $HAuCl_4$ to $NaBH_4$ were set at 1:5 and 1:10, respectively).

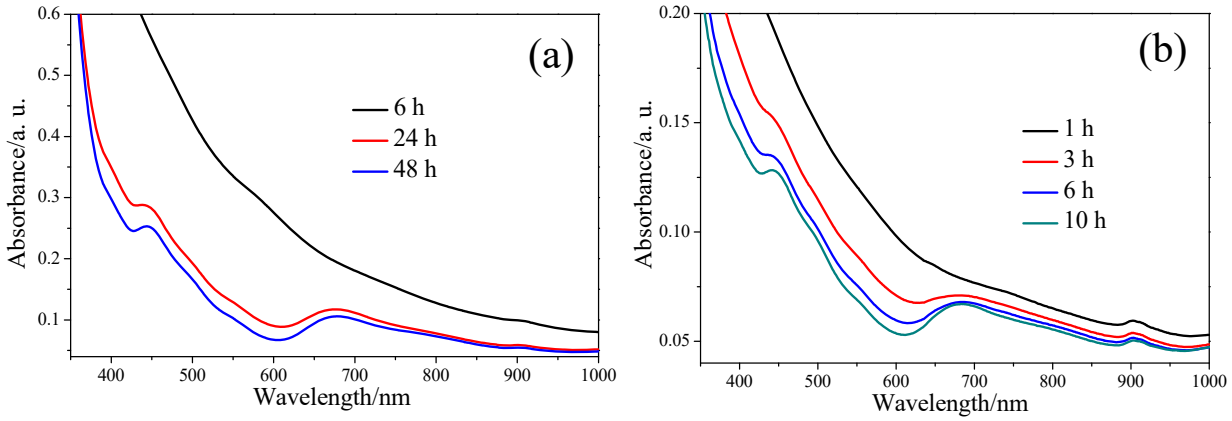

Figure S2. UV-vis absorption spectra of the crude samples in etching process: (a) $[Au_{25}(4\text{-PyET})_{18}]^-$; (b) $[Au_{25}(2\text{-PyET})_{18}]^-$.

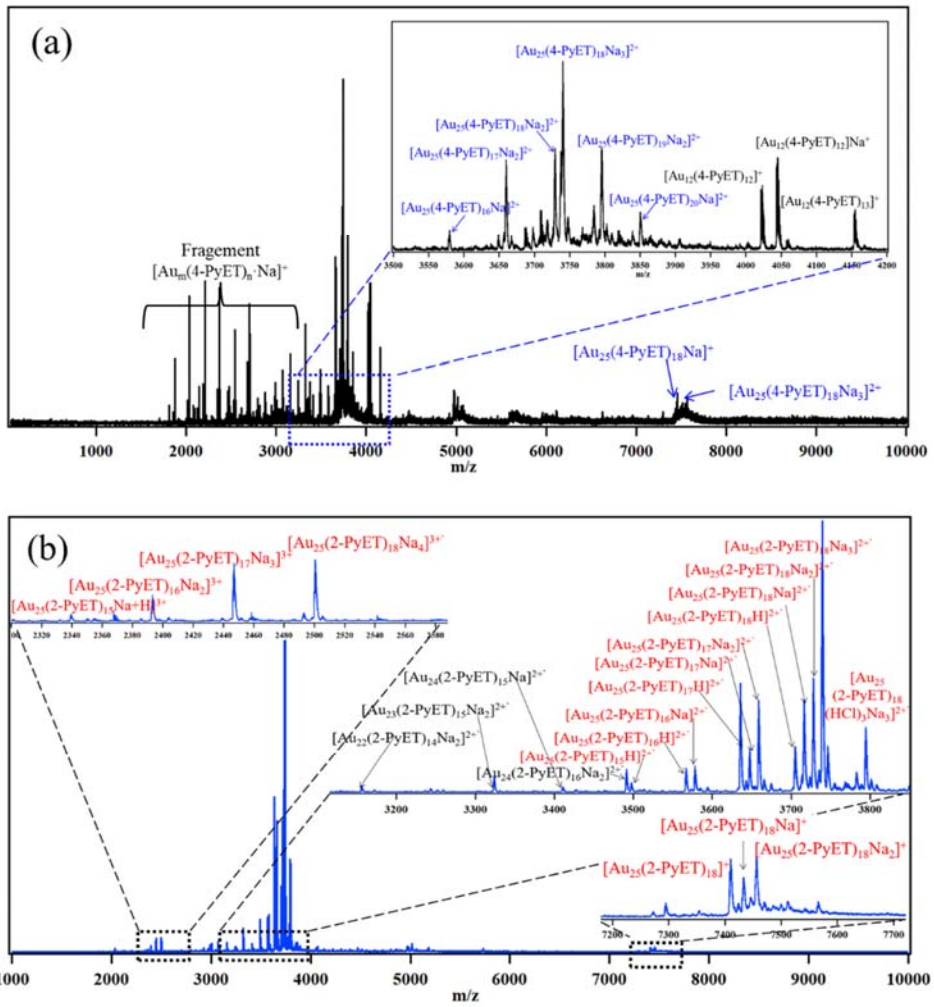

Figure S3. Positive-mode ESI mass spectra of purified $[Au_{25}(PyET)_{18}]^-$ clusters: (a) $[Au_{25}(4\text{-}PyET)_{18}]^-$; (b) $[Au_{25}(2\text{-}PyET)_{18}]^{-}\cdot$. The positive-mode ESI-MS indicated that the counterions of $[Au_{25}(PyET)_{18}]^-$ are Na^+ cation.

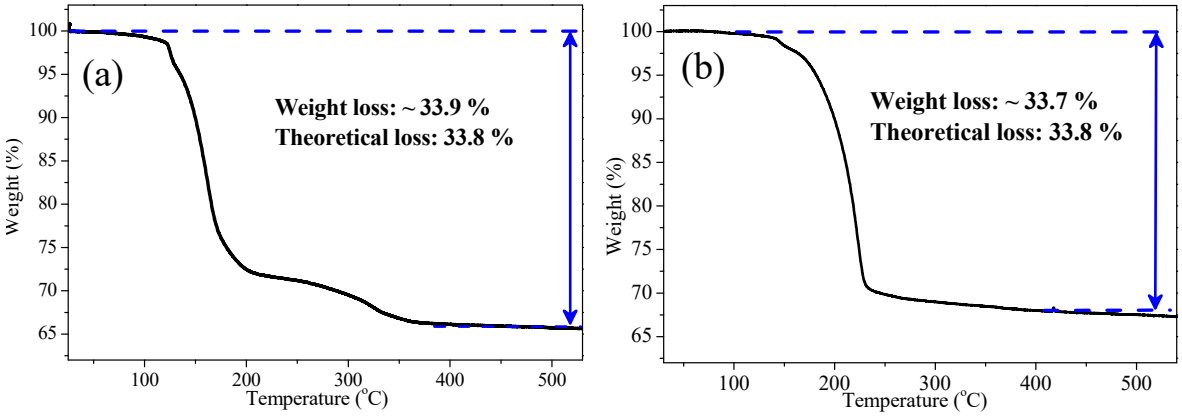

Figure S4. TGA profile of the obtained Au_{25} clusters: (a) $[Au_{25}(4\text{-PyET})_{18}]^{-}\cdot Na^{+}$; (b) $[Au_{25}(2\text{-PyET})_{18}]^{-}\cdot Na^{+}$. The purified products were used in the TGA measurements. Theoretical weight loss of $[Au_{25}(PyET)_{18}]^{-}\cdot Na^{+}$ were calculated as shown in the following Table.

	Formula weight	**Wt. (%)**
$[Au_{25}(PyET)_{18}]^{-}\cdot Na^{+}$	7434.9607	100.0
Au_{25}	4924.1638	66.2
$(PyET)_{18}\cdot Na^{+}$	2510.7969	33.8

III. Crystal results of $[Au_{25}(PyET)_{18}]^{-}\cdot Na^{+}$ and $[Au_{25}(PET)_{18}]^{-}\cdot TOA^{+}$ clusters

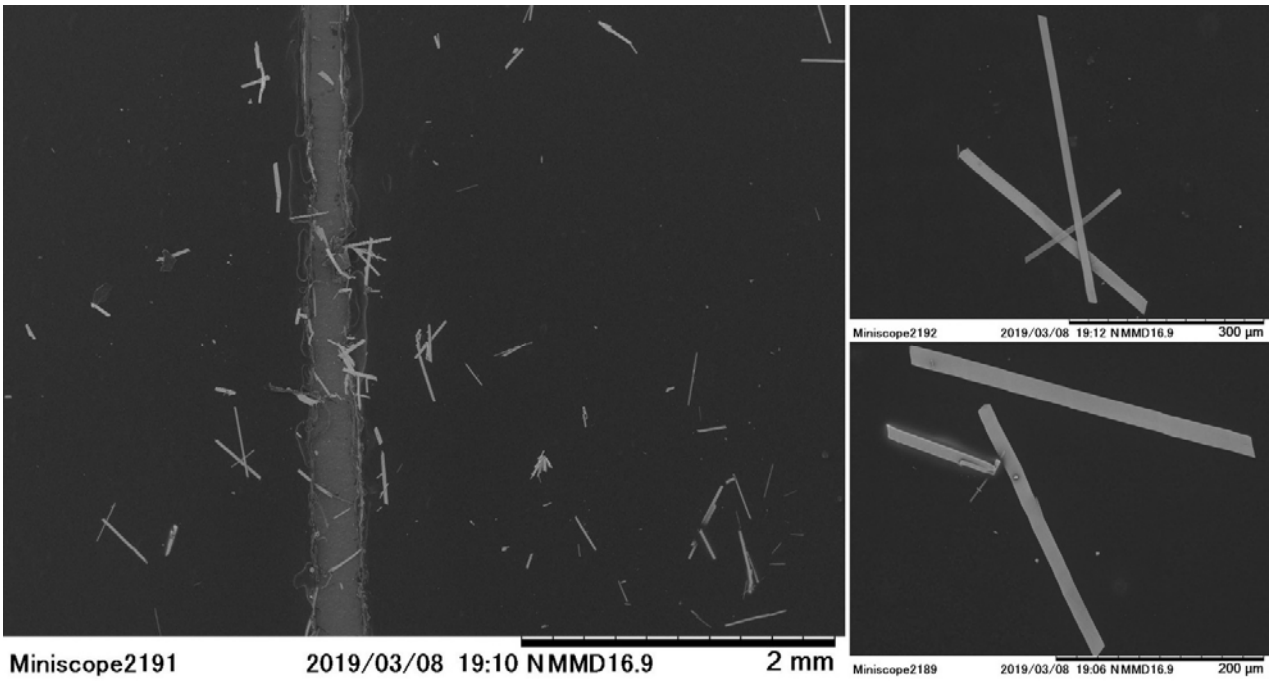

Figure S5. SEM images of the $[Au_{25}(4\text{-}PyET)_{18}]^{-}\cdot Na^{+}$ crystals.

The structure of $[Au_{25}(4\text{-}PyET)_{18}]^{-}$ cluster was solved by direct methods, and then the Na^{+} cation was located and refined by using SHELXL-2018/3 program.[S3] The pyridyl rings were restrained as a rigid hexagon with C−C distance 1.38(2) Å and C−N distance 1.32(2) Å. Idealized atom positions were calculated for all hydrogen atoms (d-(C_{methyl}−H) = 0.99 Å, d-($C_{pyridyl}$−H) = 0.95 Å). All the Au, S, N atoms and part of the C atoms were refined anisotropically. All hydrogen atoms were refined isotropically. Some of the adjacent C atoms in the pyridyl rings were restrained with effective standard deviation to have the same U_{ij} components using SIMU command. Rigid bond restraints were also applied to several pyridyl bonds using DELU command. There is one clearly disordered $-S(CH_2)_2Py$ with occupancies in the ratio of 50:50, which was refined with isotropic thermal displacement parameters. In the unit cell, the optimized occupancy value of Na^{+} cation was 0.32. Considering the −1 core charge of Au_{25} cluster, i.e. the ratio of $[Au_{25}(4\text{-}PyET)_{18}]^{-}$ to Na^{+} should be 1:1 (Figure S6), the occupancy factor of Na atom was manually set to 0.50. PLATON[S3e] was used to calculate the solvent accessible void volume and estimate the total electron count in the structure, which fit in the case to two DMF solvent molecules and six O atoms (which should be the H_2O molecules). The final residuals for the refinement were *w*R2 = 7.39%, R1 = 2.99%, GOF = 1.04 for 23712 data and 1047 parameters refined in overlapping blocks. A total of 430 restraints were applied to the refinement. All the crystal data and refinement parameters are summarized in the Table S1 and S2, respectively.

Table S1. Crystal data for Au_{25} clusters.

	$[Au_{25}(4\text{-}PyET)_{18}]^{-}\cdot Na^{+}$	**$[Au_{25}(PET)_{18}]^{-}\cdot TOA^{+}$**
Identification code	data_190405_a	data_190407_a
Empirical formula	$C_{132}H_{158}Au_{25}N_{20}NaS_{18}O_8$[a]	$C_{176}H_{162}Au_{25}NS_{18}$
Formula weight	7677.11	7792.41
Temperature/K	93(2)	93(2)
Crystal system	triclinic	triclinic
Space group	P-1	P-1
a/Å	14.4996(2)	16.0981(2)
b/Å	17.7915(3)	17.3143(3)
c/Å	19.0270(4)	18.5804(3)
α/°	85.449(2)	106.300(1)
β/°	77.874(1)	105.488(1)
γ/°	68.233(1)	90.953(1)
Volume/Å^3	4456.71(14)	4766.66(13)
Z	2	2
D_{calc}	2.848	2.715
m/mm^{-1}	20.743	19.389
F(000)	3412.0	3488.0
Crystal color, habit	black, belt	black, needle
Crystal size/mm^3	0.005×0.02×0.1	0.05×0.1×0.2

[a] Solvent molecules (DMF: $(CH_3)_2NC(O)H$×2; H_2O×6: with H atoms omitting) are involved in the lattice spaces of $[Au_{25}(4\text{-}PyET)_{18}]^{-}\cdot Na^{+}$ crystals.

Table S2. Intensity measurements and structure refinements for Au_{25} clusters.

	$[Au_{25}(4\text{-PyET})_{18}]^{-}\cdot Na^{+}$	$[Au_{25}(PET)_{18}]^{-}\cdot TOA^{+}$
Device	Rigaku VariMax Saturn	
Radiation	Mo Kα (λ = 0.71075)	
Data collection	RIGAKU CrystalClear	
2 range for data collection/°	2.092 to 29.999	1.7840 to 31.0780
Index ranges	-20 ≤ h ≤ 20, -25 ≤ k ≤ 19, -26 ≤ l ≤ 26	-22 ≤ h ≤ 22, -24 ≤ k ≤ 23, -21 ≤ l ≤ 25
Reflections collected	42372	45441
Independent reflection	23712 [R_{int} = 0.0227, R_{sigma} = 0.0330]	25390 [R_{int} = 0.0412, R_{sigma} = 0.0571]
Data/restraints/parameters	23712/430/1047	25390/1579/1094
Goodness-of-fit on F2	1.0447	1.0240
Final *R* indexes [I>=2σ (I)]	*R1* = 0.0299, *wR2* = 0.0739	*R1* = 0.0381, *wR2* = 0.0888
Final *R* indexes [all data]	*R1* = 0.0375, wR_2= 0.0779	*R1* = 0.0551, wR_2 = 0.1056
Absorption corrections	multi-scan, 0.22536 to 1.00000	multi-scan, 0.56344 to 1.00000

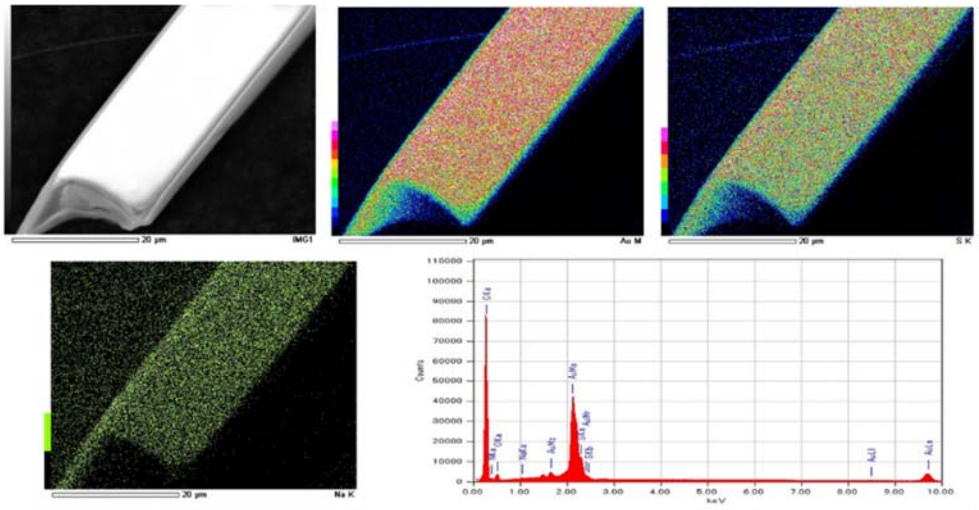

Element	Norm. At. %	Norm. At. % calculated	At. ratio	At. ratio calculated
Au	59.8	56.8	25.0	25
S	38.2	40.9	16.0	18
Na	2.0	2.3	0.83	1

Figure S6. Results of the EDX-measurement of $[Au_{25}(4\text{-PyET})_{18}]^{-}\cdot Na^{+}$ crystal. It showed an elemental ratio of Au : S : Na = 59.8 : 38.2 : 2.0, which is close to the calculated ratio for $[Au_{25}(4\text{-PyET})_{18}]^{-}\cdot Na^{+}$: 56.8 : 40.9 : 2.3.

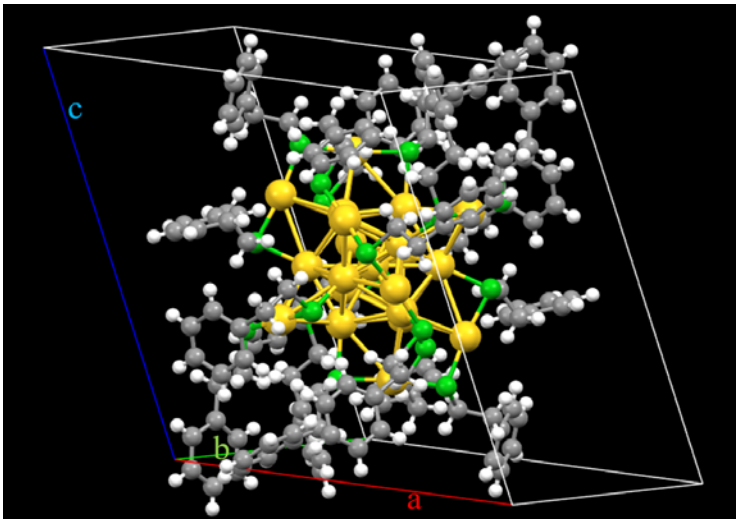

Figure S7. The crystal structure of the $[Au_{25}(PET)_{18}]^{-}\cdot TOA^{+}$ clusters (Legend: yellow, Au; green, S; grey, C; blue, N; white, H; magenta, the TOA^{+} counterion is omitted for clarity).

Table S3. Comparisons of crystallographic data, bond lengths and angles in $[Au_{25}(SR)_{18}]^-$ crystals.

Clusters		**$[Au_{25}(4\text{-PyET})_{18}]^-\cdot Na^+$**	**$[Au_{25}(PET)_{18}]^-\cdot TOA^+$**	**$[Au_{25}(PET)_{18}]^-\cdot TOA^+$**	**$[Au_{25}(PET)_{18}]^-\cdot TOA^+$**
Reference		This work	This work	*J. Am. Chem. Soc.* **2008**, *130*, 3754	*J. Am. Chem. Soc.* **2008**, *130*, 5883
***a, b, c* (Å)**		14.4996(2) 17.7915(3) 19.0270(4)	16.0981(2) 17.3143(3) 18.5804(3)	16.1114(5) 17.3313(6) 18.5810(6)	16.156(3) 17.388(3) 18.641(3)
***α, β, γ* (°)**		85.449(2) 77.874(1) 68.233(1)	106.300(1) 105.488(1) 90.953(1)	106.269(2) 105.494(2) 90.959(2)	106.359(3) 105.492(2) 90.897(3)
***V* (Å^3)**		4456.71(14)	4766.66(13)	4776.1(3)	4818.6(14)
Diameter (Å)[a]		9.84(4)	9.78(4)	9.79(4)	9.79(3)
Bond length[b] (Å)	**I**	2.76–2.79 Avg. 2.78	2.77–2.78 Avg. 2.78	2.77–2.80 Avg. 2.79	2.77–2.79 Avg. 2.78
	II	2.79–3.02 Avg. 2.92	2.79–2.97 Avg. 2.92	2.80–2.99 Avg. 2.93	2.80–2.97 Avg. 2.92
	III	3.05–3.33 Avg. 3.18	3.06–3.28 Avg. 3.16	3.03–3.24 Avg. 3.16	3.02–3.24 Avg. 3.16
	IV	2.37–2.39 Avg. 2.38	2.36–2.38 Avg. 2.37	2.37–2.40 Avg. 2.38	2.37–2.44 Avg. 2.39
	V	2.29–2.32 Avg. 2.30	2.30–2.33 Avg. 2.31	2.30–2.33 Avg. 2.31	2.23–2.32 Avg. 2.30
Bond angle[c] (°)	**∠1**	88.6 (10)	86.8 (9)	86.7 (8)	87.0 (9)
	∠2	99.7(7)	100.9 (4)	101.2 (6)	100.9 (5)

[a] The diameter of core structure of Au_{25} clusters were measured by using the average distances between the paired outermost gold atoms, see the illustration in Figure S8;

[b,c] The types of bonds and bond angles were illustrated in Figure 2C. Depictions of bonds types and bond angles in $[Au_{25}(SR)_{18}]^-$ clusters: Bond I: purple, core Au—core surface Au; Bond II: white, core surface Au—core surface Au; Bond III: red, core surface Au—motif Au; Bond IV: blue, core surface Au—motif S; Bond V: magenta, motif Au—motif S. Angle ∠1: light blue, ∠Au-S-Au, 12 S atoms that are connected to one stapled gold atom and one vertex gold atom; Angle ∠2: orange, ∠Au-S-Au, 6 S atoms that connected to two stapled golds.

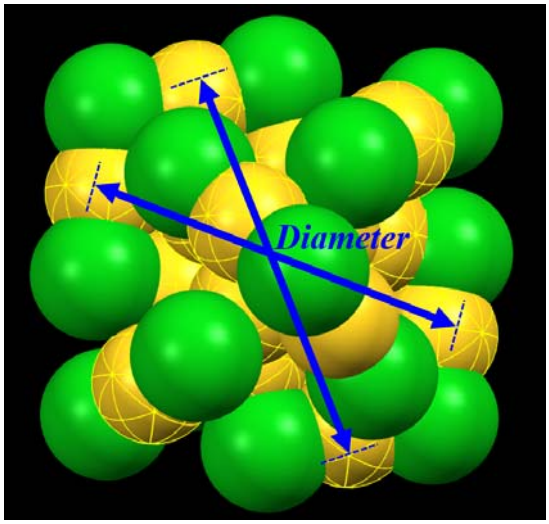

Figure S8. Illustration of the diameter of core structure in $[Au_{25}(SR)_{18}]^-$ clusters, the centroids of Au atoms were used to measure the distances between the six paired outermost Au atoms (Legend: yellow, Au; green, S; pyridyl-ethyl groups omitted for clarity).

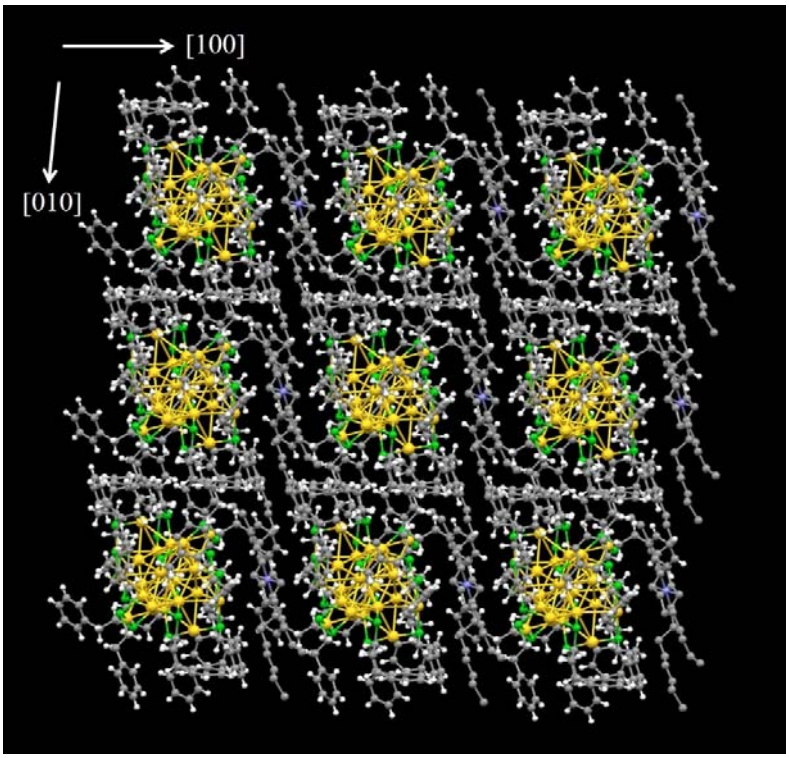

Figure S9. The view along the (001) plane of 3×3×3 superlattice in $[Au_{25}(PET)_{18}]^-\cdot TOA^+$ crystal, one disordered TOA^+ is removed for clarity (yellow, Au; green, S; grey, C; blue, N; white, H).

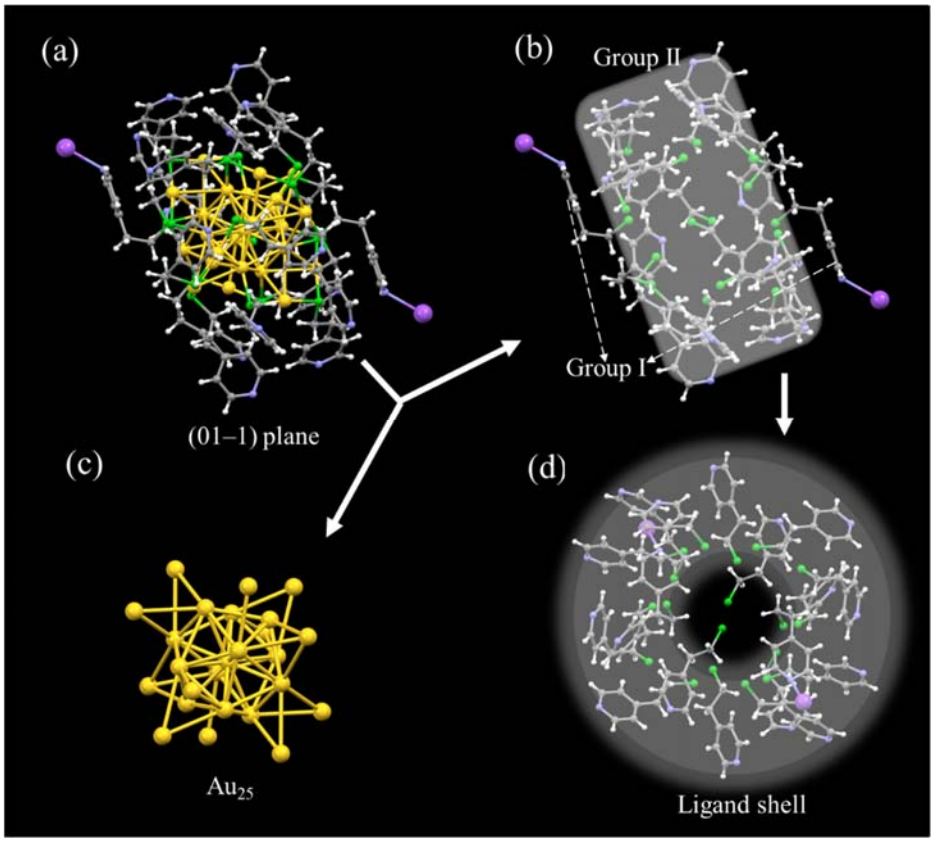

Figure S10. Crystal structure of $[Au_{25}(4\text{-PyET})_{18}]^-$ cluster: (a) the overall structure in (01–1) plane, (b) the ligand shell consisted by 18 ethylpyridyl thiolate substituents and 2 Na atoms, (c) Au_{25} consisted by Au_{13} core plus exterior 12 Au atoms, and (d) the view of ligand shell along the layered direction. Legend: yellow, Au; green, S; grey, C; blue, N; white, H; magenta, Na. It shows the ligand shell could be divided into two groups: (I) a pair of Na+-binding ethylpyridyl thiolate substituents, and (II) the other 16 ethylpyridyl thiolate substituents that forms a "ring" capping the core of cluster.

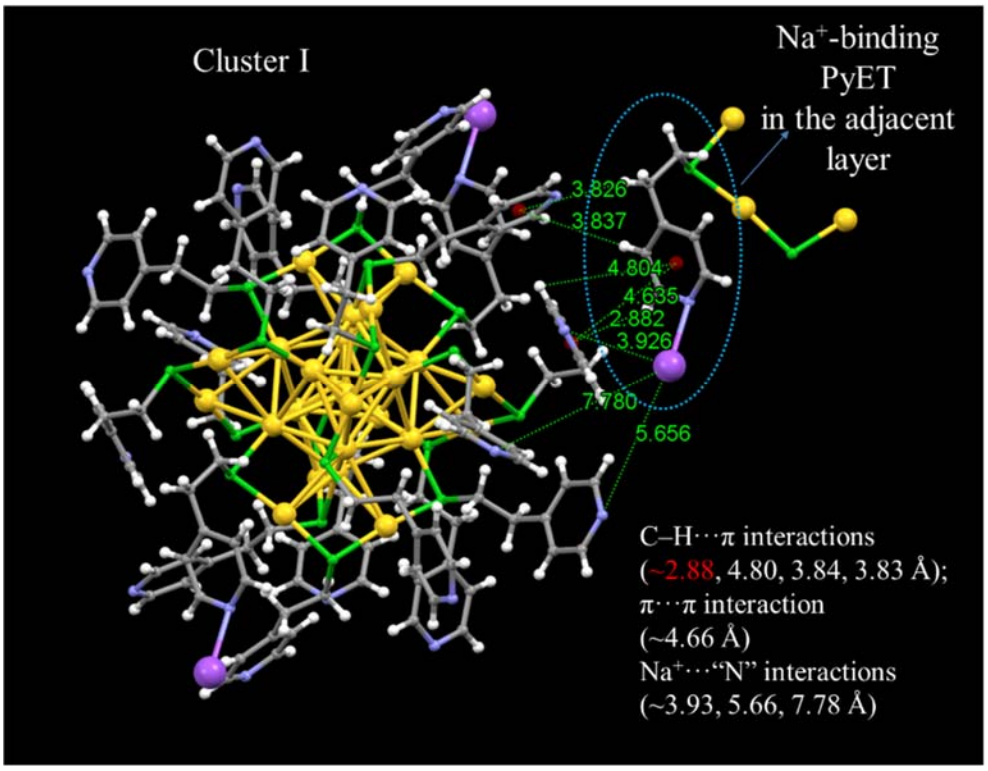

Figure S11. The interactions between the adjacent layers in $[Au_{25}(4\text{-PyET})_{18}]^{-}\cdot Na^{+}$. Legend: green, S; grey, C; blue, N; white, H; magenta, Na. It shows that except one C–H···π interaction (~2.88 Å) in the Na^{+}-binding ethylpyridyl thiolate substituents 4-PyETs (which enter its adjacent layer), the other C–H···π distances, π···π distances and Na^{+}···"N" distances are close to or larger than the sum of van der Waal radii (~3.46 Å).

IV. Titrations results of $[Au_{25}(4\text{-PyET})_{18}]^-$ clusters

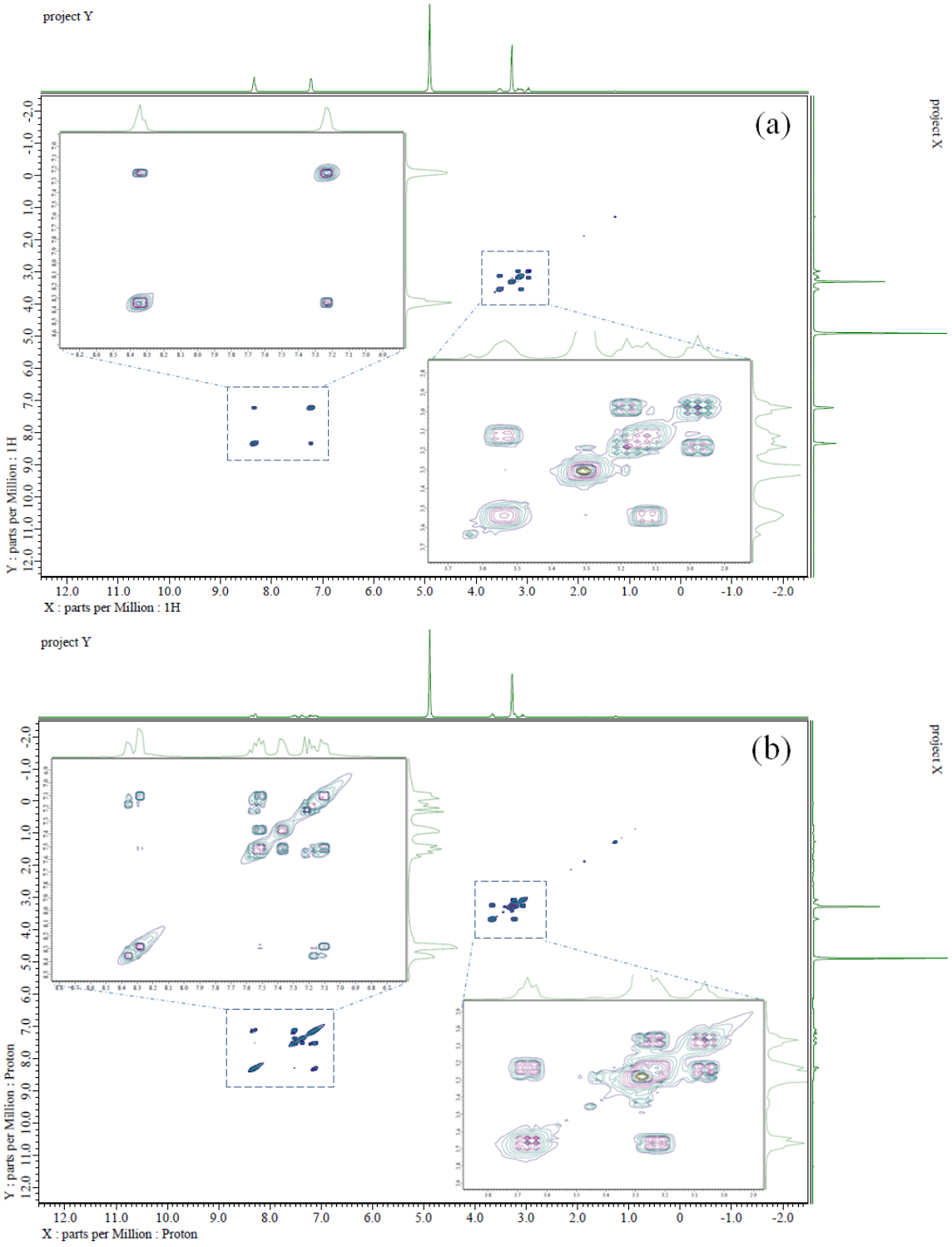

Figure S12. Full range ^{1}H-^{1}H COSY spectra of the original (a) $[Au_{25}(4\text{-PyET})_{18}]^-$; (b) $[Au_{25}(2\text{-PyET})_{18}]^-$, acquired in methanol-$d_4$.

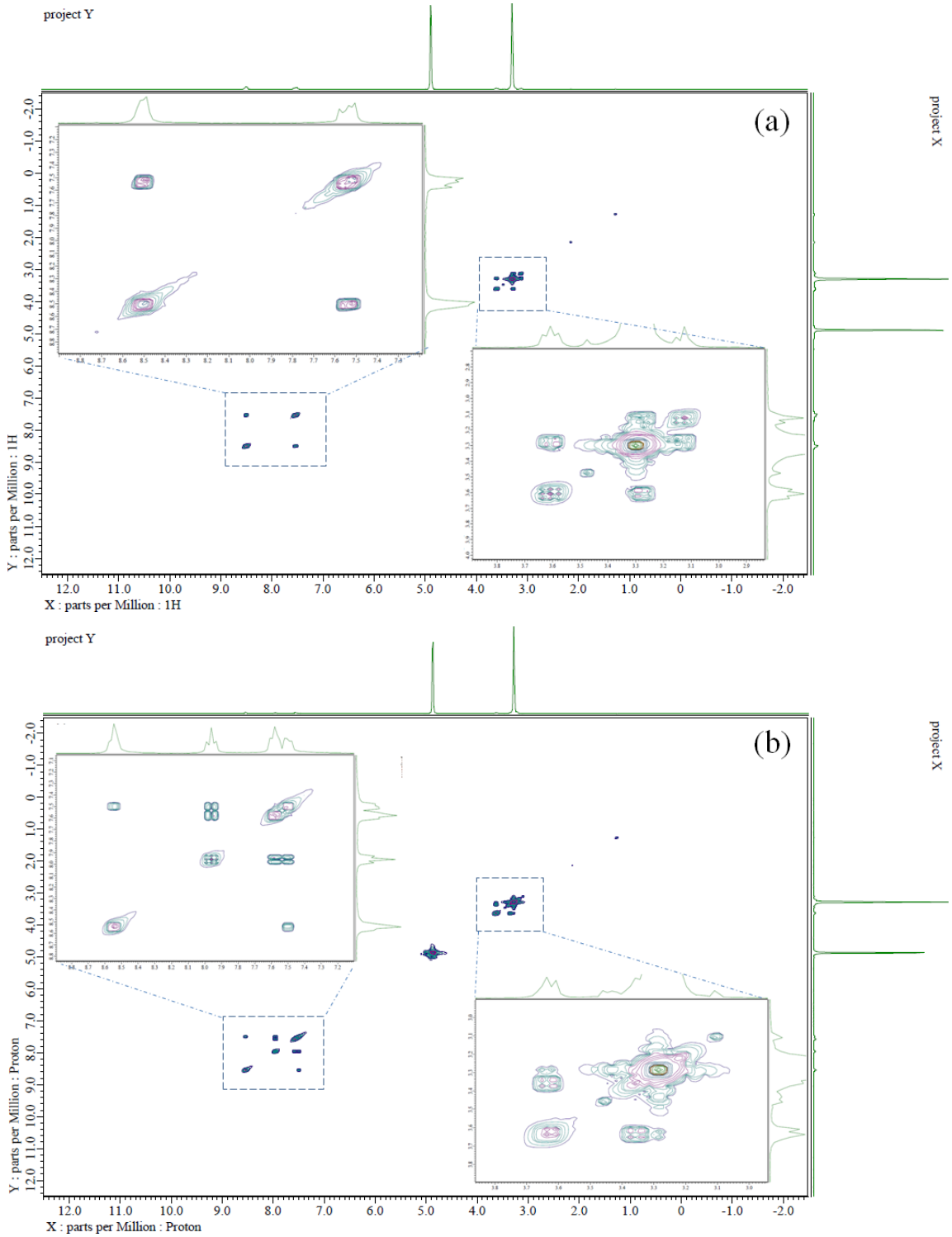

Figure S13. Full range ^{1}H-^{1}H COSY spectra of the protonated (a) $[Au_{25}(4\text{-PyET})_{18}]^{-}$; (b) $[Au_{25}(2\text{-PyET})_{18}]^{-}$, acquired in methanol-$d_4$ (0.13 μmol of $[Au_{25}(PyET)_{18}]^{-}$ clusters was dissolved in 0.6 mL of methanol-d_4, and then 16 μL of DCl-D_2O solution (50 mM) was added for protonation).

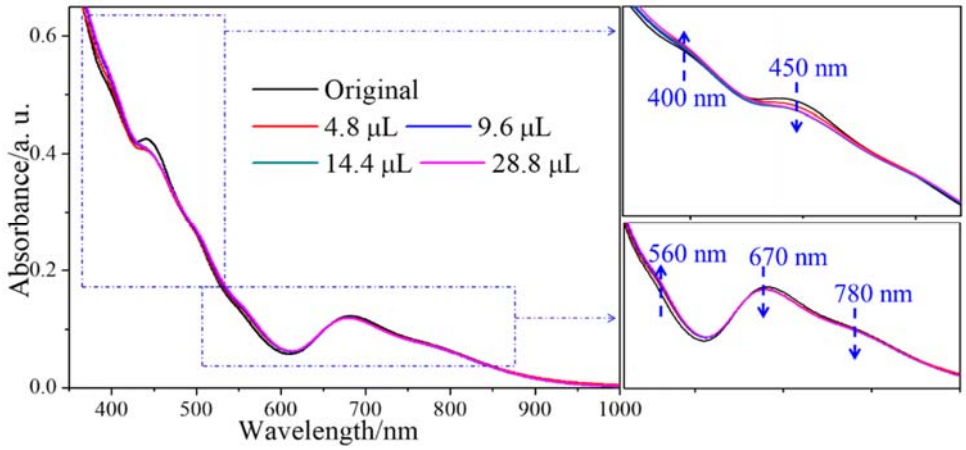

Figure S14. UV-vis absorption spectra for $[Au_{25}(2\text{-PyET})_{18}]^-$ with the addition of HCl (methanol, 500 mM). The blue arrows denote the change during the protonation. The amount of HCl required for complete protonation of $[Au_{25}(2\text{-PyET})_{18}]^-$ clusters was 9.6 μL, which was lower than that for $[Au_{25}(4\text{-PyET})_{18}]^-$ clusters of 14.4 μL.

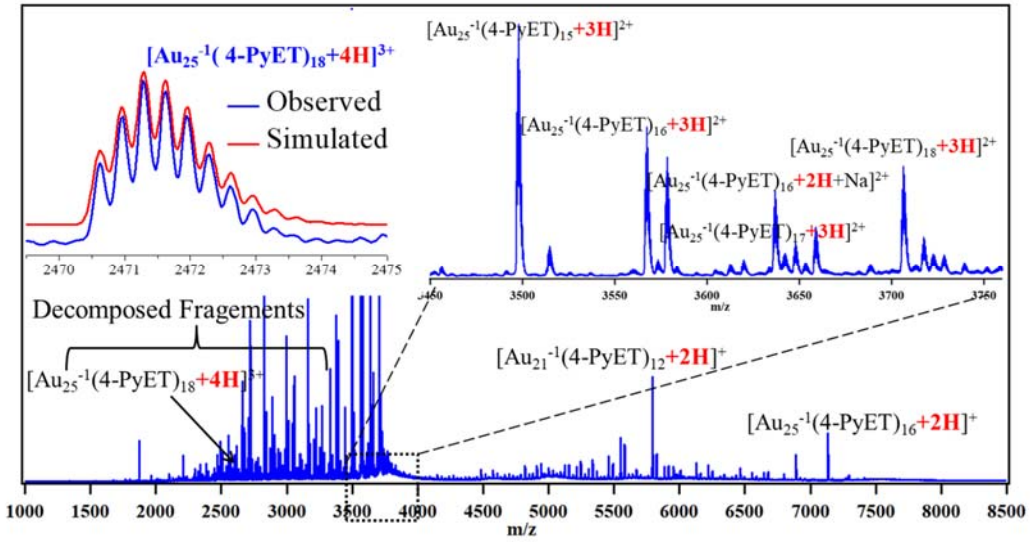

Figure S15. Positive-mode ESI mass spectrum of the $[Au_{25}(4\text{-PyET})_{18}]^-$ clusters with the addition of HCl-methanol solution.

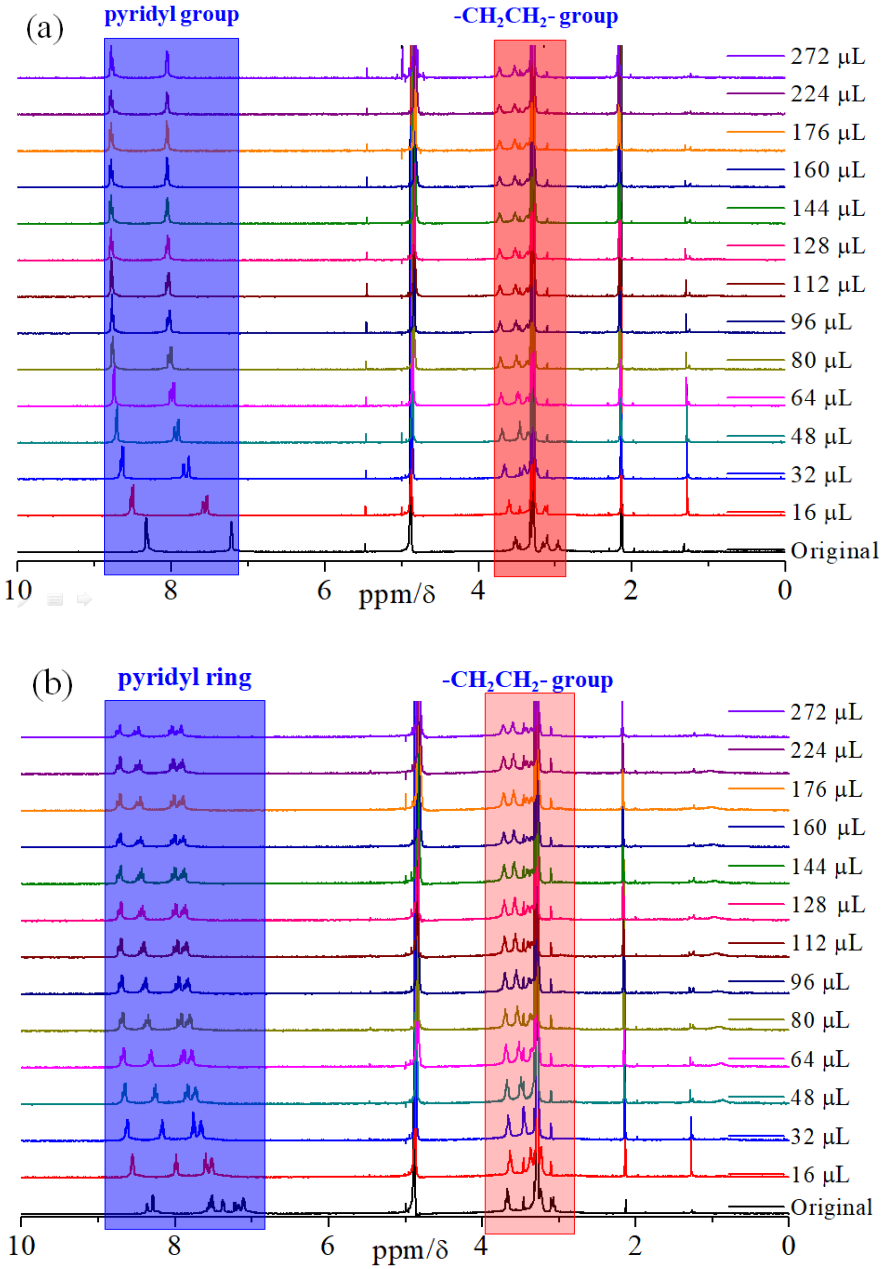

Figure S16. ^{1}H-NMR spectra of (a) $[Au_{25}(4\text{-PyET})_{18}]^{-}$, (b) $[Au_{25}(2\text{-PyET})_{18}]^{-}$ upon titration of DCl-D_2O (50 mM), acquired in methanol-d_4.

Table S4. ^{1}H-NMR chemical shifts (δ) of (a) $[Au_{25}(4\text{-PyET})_{18}]^{-}$; (b) $[Au_{25}(2\text{-PyET})_{18}]^{-}$ with the protonation of the pendant PyET in Figure S16.

(a) $[Au_{25}(4\text{-PyET})_{18}]^{-}$								
DCl amount	***α*-CH$_2$**		***β*-CH$_2$**		***o*-CH**		***m*-CH**	
	Inner	*Outer*	*Inner*	*Outer*	*Inner*	*Outer*	*Inner*	*Outer*
Original	3.52	3.16	3.16	2.96	8.33	8.30	7.21	7.21
16 μL	3.60	n. d[a]	n. d.	n. d.	8.50	8.53	7.53	7.59
32 μL	3.66	n. d.	n. d.	n. d.	8.64	8.66	7.77	7.83
48 μL	3.68	n. d.	3.46	n. d.	8.71	8.72	7.90	7.96
64 μL	3.70	n. d.	3.47	n. d.	8.74	8.74	7.97	8.01
80 μL	3.71	3.37[b]	3.50	n. d.	8.76	8.76	8.00	8.03
96 μL	3.71	3.37[b]	3.51	n. d.	8.77	8.77	8.02	8.05
112 μL	3.72	3.37[b]	3.52	n. d.	8.78	8.78	8.03	8.06
128 μL	3.72	3.37[b]	3.52	n. d.	8.78	8.78	8.04	8.06
144 μL	3.72	3.37[b]	3.52	n. d.	8.78	8.78	8.05	8.06
160 μL	3.72	3.37[b]	3.52	n. d.	8.78	8.78	8.06	8.06
176 μL	3.72	3.37[b]	3.52	n. d.	8.78	8.78	8.06	8.06
224 μL	3.72	3.37[b]	3.52	n. d.	8.78	8.78	8.06	8.06
272 μL	3.72	3.37[b]	3.52	n. d.	8.78	8.78	8.06	8.06

(b) $[Au_{25}(2\text{-PyET})_{18}]^-$												
DCl amount	***α*-CH₂**		***β*-CH₂**		***1*-CH**		***2*-CH[c]**		***3*-CH[c]**		***4*-CH**	
	Inner	*Outer*	*Inner*	*Outer*	*Inner*	*Outer*	*Inner*	*Outer*	*Inner*	*Outer*	*Inner*	*Outer*
Original	3.62	3.26[b]	3.26[b]	3.09	7.37	7.22	7.52	7.56	7.11	7.17	8.29	8.36
16 μL	3.64	3.37[b]	n. d.	3.23b	7.60	7.60	7.99	7.99	7.52	7.52	8.54	8.54
32 μL	3.66	3.45[b]	n. d.	n. d.	7.76	7.76	8.16	8.16	7.66	7.66	8.62	8.64
48 μL	3.67	3.49[b]	n. d.	n. d.	7.83	7.86	8.25	8.25	7.73	7.73	8.65	8.67
64 μL	3.69	3.52[b]	n. d.	n. d.	7.88	7.92	8.31	8.31	7.79	7.79	8.66	8.70
80 μL	3.70	3.54[b]	n. d.	3.36[b]	7.91	7.95	8.36	8.36	7.81	7.81	8.68	8.71
96 μL	3.70	3.55[b]	n. d.	3.38[b]	7.94	7.98	8.39	8.39	7.83	7.83	8.69	8.72
112 μL	3.71	3.56	n. d.	3.39[b]	7.96	8.01	8.42	8.42	7.86	7.86	8.69	8.73
128 μL	3.71	3.57	n. d.	3.40[b]	7.99	8.03	8.44	8.44	7.88	7.88	8.7	8.74
144 μL	3.71	3.58	n. d.	3.41[b]	8.00	8.04	8.44	8.44	7.88	7.88	8.7	8.74
160 μL	3.71	3.58	n. d.	3.41[b]	8.00	8.04	8.44	8.44	7.88	7.88	8.7	8.75
176 μL	3.71	3.58	n. d.	3.41[b]	8.00	8.04	8.44	8.44	7.88	7.88	8.7	8.75
224 μL	3.71	3.58	n. d.	3.41[b]	8.00	8.04	8.44	8.44	7.88	7.88	8.71	8.75
272 μL	3.71	3.58	n. d.	3.41[b]	8.00	8.04	8.44	8.44	7.88	7.88	8.71	8.75

[a] n. d.= not determined because the overlaps with the solvent signals; [b] partially overlaps with solvent signals; [c] hard to assign the inner and outer sites separately.

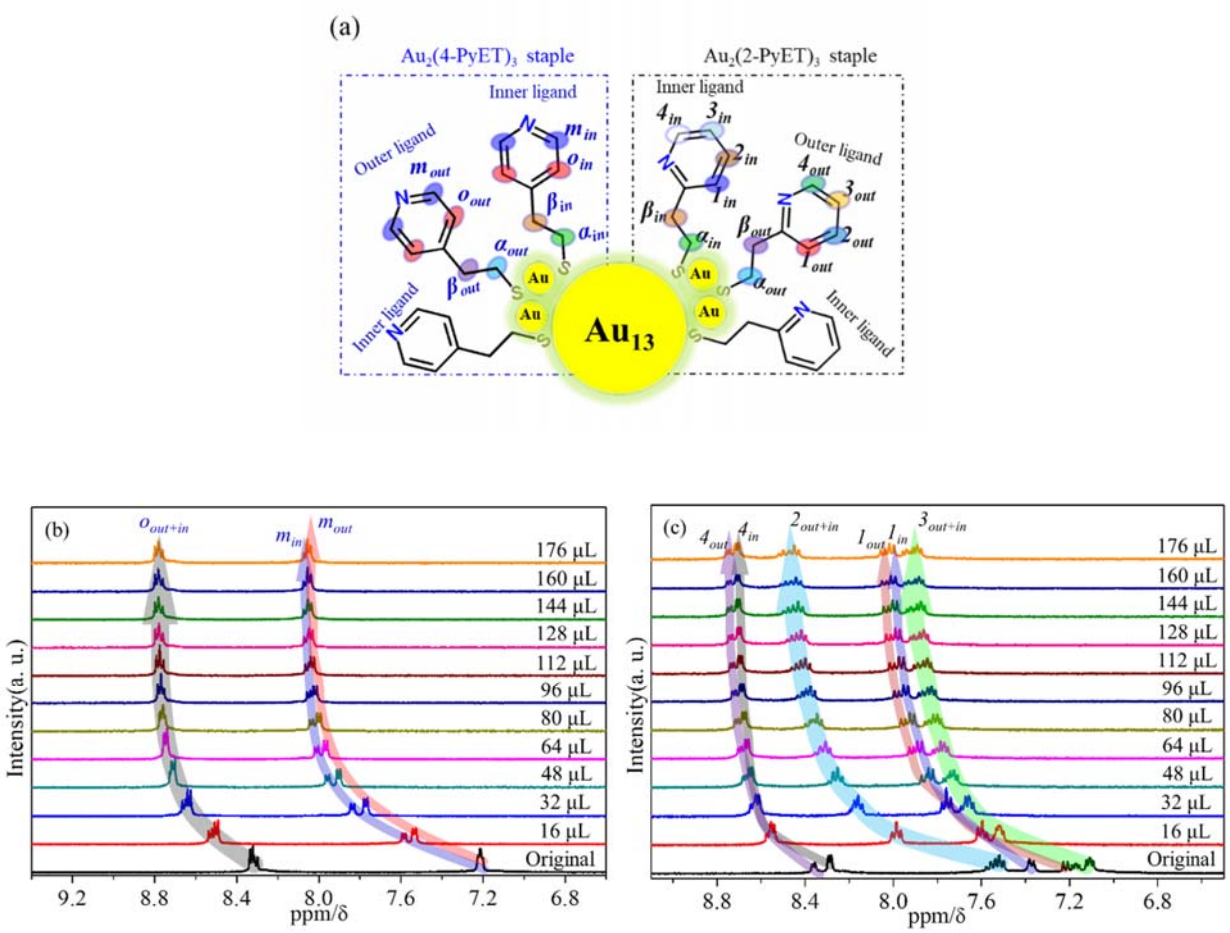

Figure S17. Schematic (a) of the dimeric staples (Au_2PyET_3) on $[Au_{25}(PyET)_{18}]^-$ surface, ^{1}H-NMR spectra of the Py protons in (b) $[Au_{25}(4\text{-}PyET)_{18}]^-$; (c) $[Au_{25}(2\text{-}PyET)_{18}]^-$ on addition of DCl-D_2O (50 mM), acquired in methanol-d_4. The structure of the $[Au_{25}(PyET)_{18}]^-$ clusters consisted of an icosahedral Au_{13} kernel and six $Au_2(PyET)_3$ motifs (Figure 2). Therefore, there were two different chemical environments for the 18 PyET ligands, i.e., the inner ligands and outer ligands that were present in a ratio of 2:1 (Figure S17a).[S4] The peak assignments were verified by their corresponding ^{1}H-^{1}H COSY spectra (Figure S12 and S13). As shown in Figure S17b, the ^{1}H signals of *o* and *m* are from the *o*-position (*othor-* to the N center) and *m*-position (*meta-* to the N center) of Py-group, respectively, α corresponding to the α-CH_2 group (closest to the −S−), β corresponding to the β-CH_2 group (second closest to −S−). The same peak assignments of the pendant 2-PyET could be summarized as: α-CH_2 group, β-CH_2 group, *1*-CH, *2*-CH, *3*-CH and *4*-CH. (Figure S17c) The subscripts "*in*" and "*out*" represent the inner PyET" and outer PyET, respectively.

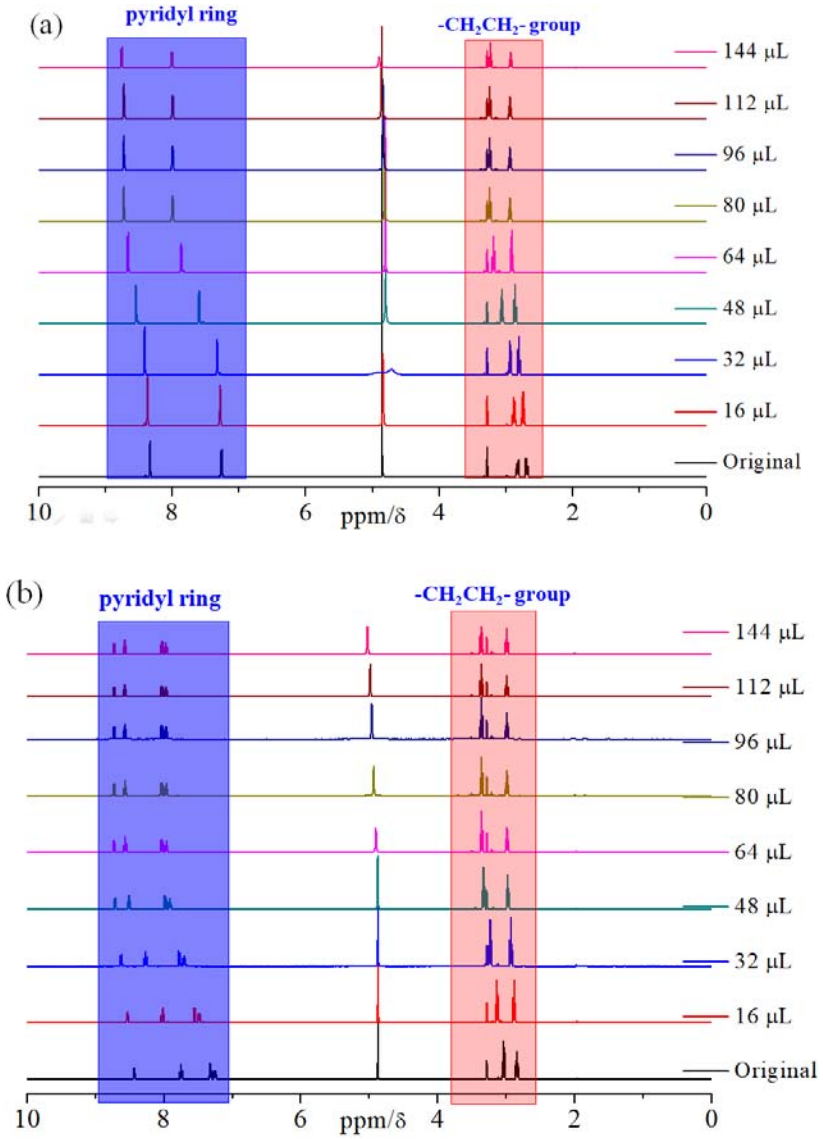

Figure S18. ^{1}H-NMR spectra of (a) 4-PyET, (b) 2-PyET upon titration of DCl-D_2O (50 mM), acquired in methanol-d_4. Of note, the masses for titrations of free PyET ligands were same as the corresponding PyET on $[Au_{25}(PyET)_{18}]^{-}$ surfaces. The original 4-PyET·HCl was first neutralized by NaOD and then the titration was conducted. The peak assignments were verified by their corresponding ^{1}H-^{1}H COSY spectra (Figure S19).

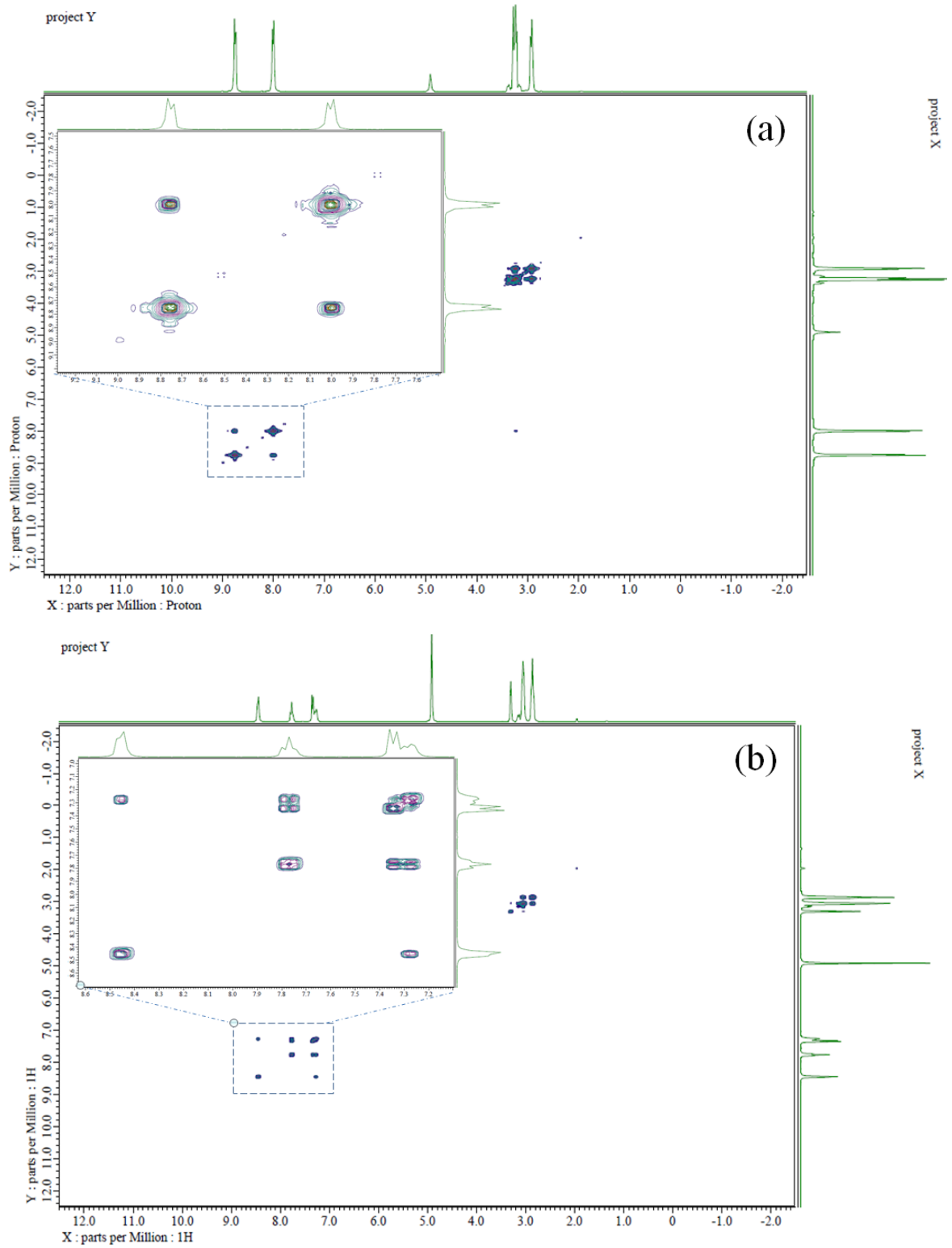

Figure S19. ^{1}H-^{1}H COSY spectra of the original (a) 4-PyET·HCl; (b) 2-PyET acquired in methanol-d_4.

Table S5. ^{1}H-NMR chemical shifts (δ) of (a) 4-PyET; (b) 2-PyET upon titration of DCl-D_2O (50 mM) in Figure S18.

(a) 4-PyET				
DCl amount	***α-CH₂***	***β-CH₂***	***o-CH***	***m-CH***
Original	2.83	2.70	7.26	8.34
16 μL	2.88	2.74	7.28	8.37
32 μL	2.94	2.81	7.42	8.45
48 μL	3.07	2.86	7.60	8.54
64 μL	3.19	2.91	7.87	8.67
80 μL	3.24	2.94	7.99	8.72
96 μL	3.24	2.94	8.00	8.73
112 μL	3.24	2.94	8.00	8.73
144 μL	3.24	2.94	8.00	8.73

(b) 2-PyET						
DCl amount	***α-CH₂***	***β-CH₂***	***1-CH***	***2-CH***	***3-CH***	***4-CH***
Original	3.04	2.84	7.32	7.75	7.25	8.43
16 μL	3.13	2.89	7.55	8.02	7.48	8.53
32 μL	3.23	2.93	7.77	8.27	7.70	8.62
48 μL	3.33	2.97	7.98	8.51	7.91	8.71
64 μL	3.36	2.99	8.02	8.57	7.96	8.73
80 μL	3.36	2.99	8.02	8.57	7.96	8.73
96 μL	3.36	2.99	8.02	8.57	7.96	8.73
112 μL	3.36	2.99	8.02	8.57	7.96	8.73
144 μL	3.36	2.99	8.02	8.57	7.96	8.73

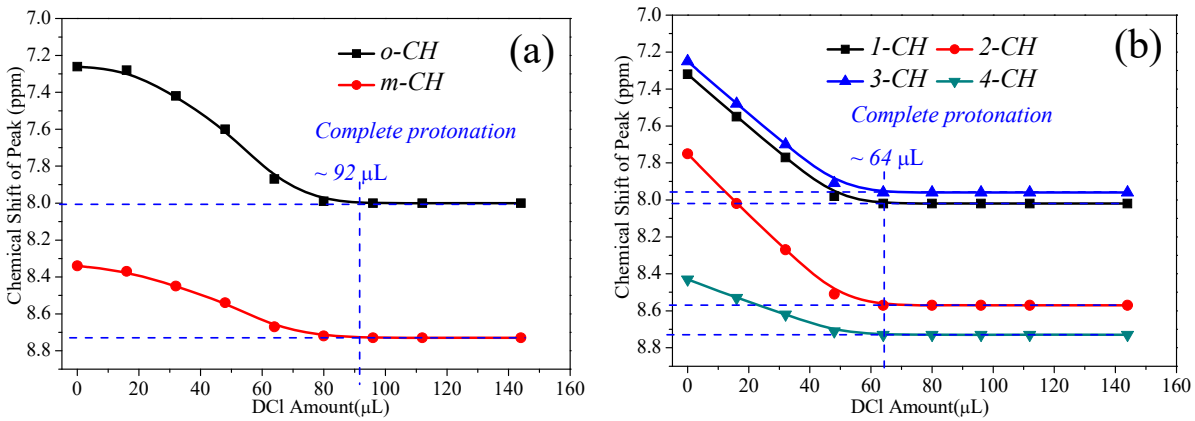

Figure S20. ^{1}H-NMR chemical shifts in ppm for Py protons in (a) 4-PyET and (b) 2-PyET as a function of amount of DCl. The proton signals of the Py moiety shifted more downfield upon titration by DCl. The H^+-binding affinity of free 4-PyET was weaker than that of free 2-PyET, as indicated by their critical H^+ concentrations (~6.6 × 10^{-3} M for 4-PyET against ~4.8 × 10^{-3} M for 2-PyET for complete protonation; Table 1, entries 3–4). These data demonstrate that not only the NMR shifts but also H^+-binding activities are affected by the relative position of the N center in Py-groups.

V. Reversible (de)protonation of $[Au_{25}(PyET)_{18}]^-$ clusters

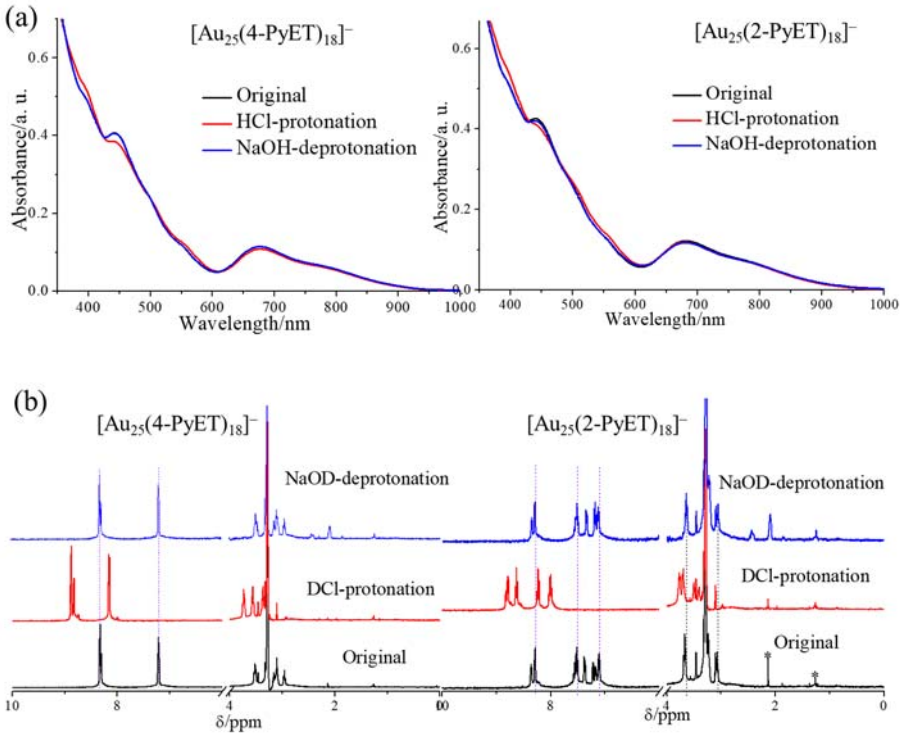

Figure S21. Reversible protonation reaction on $[Au_{25}(PyET)_{18}]^-$ clusters: (a) UV-vis absorption; and (b) ^{1}H-NMR spectra.

Table S6. Solubility of $[Au_{25}(PET)_{18}]^{-}$, and $[Au_{25}(PyET)_{18}]^{-}$ clusters in protonated and deprotonated states.

Solvent	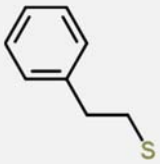	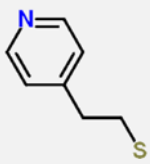	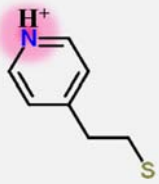	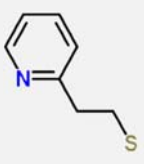	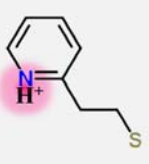
H_2O	I	I	$S^{+[a]}$	I	$S^{+[a]}$
Alcohol	I	S^{+}	S^{+}	S^{+}	S^{+}
DMF	S^{+}	S^{+}	S^{+}	S^{+}	S^{+}
THF	S^{+}	S^{-}	$I^{[a]}$	S	$I^{[a]}$
THF-MeOH (Vol., 3:1)	I	S^{+}	$I^{[a]}$	S^{+}	$I^{[a]}$
Toluene	S^{+}	I	$S^{[b]}$	I	$S^{[b]}$
DCM	S^{+}	I	$S^{[b]}$	S	$S^{-[b]}$
MeCN	S	S^{-}	$S^{[a,b]}$	S^{-}	$S^{[a,b]}$
Acetone	S	S^{-}	$S^{[a,b]}$	S^{-}	$S^{[a,b]}$
Hexane	I	I	$I^{[b]}$	I	$I^{[b]}$
Ether	I	I	$I^{[b]}$	I	$I^{[b]}$

[a] Aq. HCl (375 mM, 20 µL) was added for protonation; [b] Acetic acid (20 µL) was added for protonation;

[c] Solubility: $S^{+} > S > S^{-}$, Insoluble: I; [d] In each batch, ~ 1.0 mg of Au_{25} clusters was tested in 1.0 mL of the solvent.

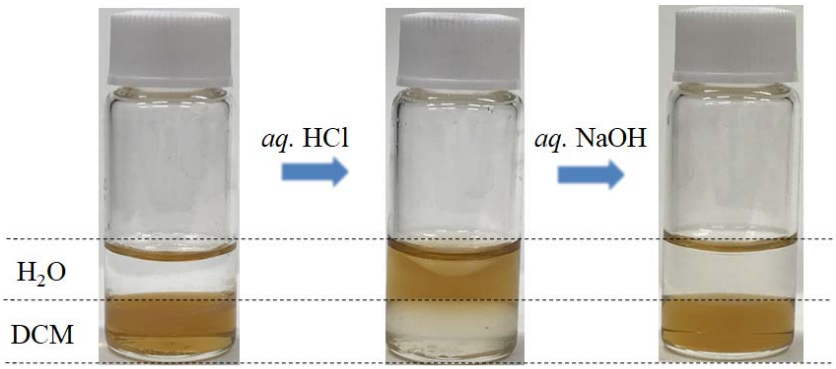

Figure S22. Transfer noted for $[Au_{25}(2\text{-}PyET)_{18}]^{-}$ clusters between aqueous and organic (DCM, dichloromethane) media through protonation–deprotonation process.

VI. References

[S1] J. F. Parker, J. E. Weaver, F. McCallum, C. A. Fields−Zinna, R. W. Murray, *Langmuir* **2010**, *26*, 13650−13654.

[S2] M. Zhu, C. M. Aikens, F. J. Hollander, G. C. Schatz, R. Jin, *J. Am. Chem. Soc.* **2008**, *130*, 5883−5885.

[S3] a) G. M. Sheldrick, *Acta Cryst.* **2008**, *A64*, 112−122; b) G. M. Sheldrick, *Acta Cryst.* **2015**, *A71*, 3−8; c) G. M. Sheldrick, T. R. Schneider, *Methods Enzymol.* **1997**, *277*, 319−343; b) G. M. Sheldrick, *Acta Cryst.* **2015**, *C71*, 3−8; e) A. L. Spek, *Acta Cryst.* **2015**, *C71*, 9−18.

[S4] a) A. Venzo, S. Antonello, J. A. Gascón, I. Guryanov, R. D. Leapman, N. V. Perera, A Sousa, M. Zamuner, A. Zanella, F. Maran, *Anal. Chem.* **2011**, *83*, 6355−6362; b) H. Qian, M. Zhu, C. Gayathri, R. R. Gil, R. Jin, *ACS Nano* **2011**, *5*, 8935−8942.